Journal of Power Sources 225 (2013) 263–268

Contents lists available at SciVerse ScienceDirect

Journal of Power Sources

journal homepage: www.elsevier.com/locate/jpowsour

Short communication

Photoelectrochemical cell/dye-sensitized solar cell tandem water splitting systems with transparent and vertically aligned quantum dot sensitized TiO_2 nanorod arrays

Kahee Shin [a], Ji-Beom Yoo [b], Jong Hyeok Park [a,*]

[a] School of Chemical Engineering and SAINT, Sungkyunkwan University, Suwon 440-746, Republic of Korea
[b] School of Advanced Materials Science and Engineering and SAINT, Sungkyunkwan University, Suwon 440-746, Republic of Korea

HIGHLIGHTS

- To realize an unassisted water splitting system, the photoanode and dye-sensitized solar cell tandem structures are tried.
- Vertically aligned CdS sensitized TiO_2 nanorod arrays are grown on transparent conducting oxide substrate.
- Electrodeposition and spray pyrolysis deposition of CdS nanoparticle sensitization are carried out.

GRAPHICAL ABSTRACT

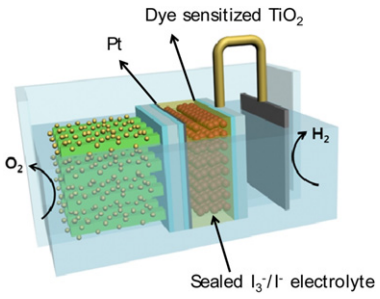

ARTICLE INFO

Article history:
Received 28 July 2012
Received in revised form
17 September 2012
Accepted 12 October 2012
Available online 27 October 2012

Keywords:
Water splitting
Tandem
Photoanode
Photocurrent
Nanorod

ABSTRACT

The present work reports fabrication of vertically aligned CdS sensitized TiO_2 nanorod arrays grown on transparent conducting oxide substrate with high transparency as a photoanode in photoelectrochemical cell for water splitting. To realize an unassisted water splitting system, the photoanode and dye-sensitized solar cell tandem structures are tried and their electrochemical behaviors are also investigated. The hydrothermally grown TiO_2 nanorod arrays followed by CdS nanoparticle decoration can improve the light absorption of long wavelength light resulting in increased photocurrent density. Two different techniques (electrodeposition and spray pyrolysis deposition) of CdS nanoparticle sensitization are carried out and their water splitting behaviors in the tandem cell are compared.

1. Introduction

As the importance of clean and renewable energy production has been on the increase, worldwide research has been focused on the energy conversion devices such as photovoltaics, batteries and fuel cells. Since the photoelectrochemical (PEC) splitting of water with a titanium dioxide (TiO_2) semiconductor reported by Fujishima and Honda [1], solar hydrogen generation is considered one of the best ways of energy production due to the infinite amount of solar energy and water without emission of pollutants. Since then, many studies have been reported on solar water splitting based on various kinds of materials, especially metal oxides such as TiO_2, ZnO, WO_3 and Fe_2O_3 [2–9]. Of the materials being studied as a potential photoanode, TiO_2 has been considered the best material due to its low cost and photochemical stability [10,11].

* Corresponding author. Tel.: +82 31 290 7346; fax: +82 31 290 7272.
E-mail addresses: lutts@skku.edu, anotherpark@gmail.com (J.H. Park).

0378-7753/$ – see front matter © 2012 Elsevier B.V. All rights reserved.
http://dx.doi.org/10.1016/j.jpowsour.2012.10.036

To achieve a better photoelectrochemical response with these materials, an extensive research has been done on controlling its nanostructure [12–17]. Aligned one dimensional (1D) nanostructures such as nanotubes, nanowires and nanorods have received considerable attention because of their outstanding electron transport mobility [18]. Studies on TiO_2 nanotubes obtained by anodizing of Ti metal have been carried out extensively since the process is easier and cheaper than other techniques. In spite of its better physical property, there is a limitation of application in photoelectrochemical cell owing to its opaque property, which obstructs the application of the TiO_2 nanotube arrays to the PEC/dye-sensitized solar cell (DSSC) tandem cell for unassisted water splitting. Recently, Liu et al. reported the synthesis method for single-crystalline TiO_2 nanorods on transparent conducing oxide (TCO) substrate using the hydrothermal method [19]. However, one of the limiting factors of this material as a photoanode is its large bandgap, resulting photon-absorption of only the UV region of the solar spectrum. Fortunately, coupling small bandgap materials with TiO_2 (e.g., CdS [20,21], CdSe [22–24]) can extend light absorption to the visible region. Following a research paper written by Misra et al., CdS nanoparticles can be synthesized directly onto 1D TiO_2 nanotubes with an electrochemical method [25]. Moreover, our previous paper reported about the synthesis of CdS nanoparticles on the surface of TiO_2 nanotubes using spray pyrolysis deposition which resulted in the highly efficient photoanode in PEC cell [26].

In this work, we report on an inquiry on CdS nanoparticles decorated TiO_2 nanorod arrays on the TCO substrate from not only the electrodeposition method but also the spray pyrolysis deposition method, respectively (Fig. 1(a)). The comparison study on the photoelectrochemical performances of each photoanode from two different deposition methods was also demonstrated. Furthermore, PEC/DSSC tandem cell (Fig. 1(b)) was fabricated to attain an unassisted water splitting system, thanks to its high transparency.

2. Experimental

2.1. Synthesis of TiO_2 nanorod arrays

The TiO_2 nanorod arrays were fabricated from a hydrothermal method [19]. The fluorine doped tin oxide (SnO_2:F) (FTO) glass substrate had been cleaned by ultrasonicating in acetone, isopropanol and methanol for 10 min each, followed by rinsing in de-ionized (DI) water and drying in N_2 gas. In a typical synthesis process, the substrates with the buffer layer are placed within sealed Teflon-lined autoclaves (63 mL), containing 20 mL of hydrochloric acid (37 wt%), 20 mL of DI water and 0.5 g of titanium isopropoxide. The solutions were then heated at 120 °C for 11 h. After the reaction period, the films were rinsed with DI water and dried at room temperature.

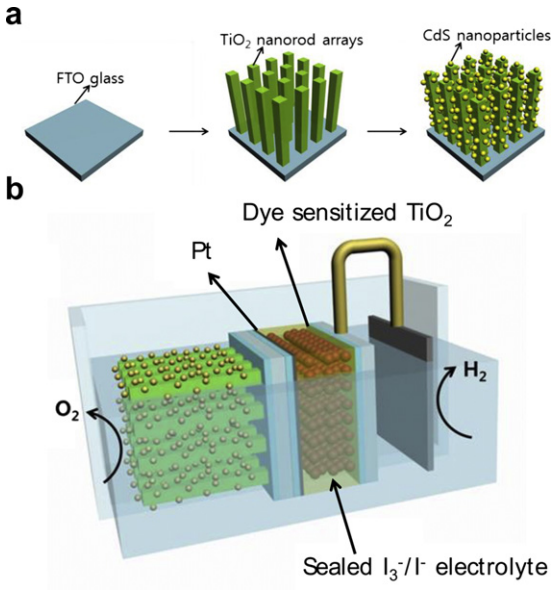

Fig. 1. Schematic diagram of (a) the process used for CdS nanoparticles coated on TiO_2 nanorod arrays and (b) PEC/DSSC tandem cell.

2.2. Deposition of CdS nanoparticles on TiO_2 nanorod arrays

The depositions of CdS were performed by two different methods namely electrodeposition and spray pyrolysis deposition. In the case of electrodeposition, 0.2 M $CdCl_2$ and 0.05 M $Na_2S_2O_3$ containing aqueous solution of pH controlled at ~2.1 using 0.1 N of HCl was prepared as a precursor solution [25]. The synthetic TiO_2 nanorod arrays were immersed in the heated solution at 50 °C, applied voltage of −0.8 V vs. standard calomel electrode (SCE) for 1000 s. After the electrochemical reaction, the sample was washed with DI water, dried at room temperature and sintered at 500 °C for 6 h in air condition. For the spray pyrolysis deposition of CdS nanoparticles, the aqueous solution of 0.1 M $CdCl_2$ and 0.1 M thiourea was used as a precursor and the TiO_2 nanorod arrays were preheated to 450 °C. In that case, 0.8 mL of the precursor solutions were sprayed for 2 s and were left for 10 s for the formation of CdS on the TiO_2 nanorod layer, making this as 1 cycle. For the sufficient incubation of CdS on the TiO_2 nanorods, we repeated the spray pyrolysis deposition process 5 times.

2.3. Tandem cell fabrication

An anatase single-layered TiO_2 mesoporous film was used as a photoanode of the DSSC. A 8 μm thick TiO_2 nanoparticle film was coated on a pretreated FTO glass substrate by applying UV with a 100 mM $TiCl_4$ solution. After annealing at 500 °C for 30 min, the nanocrystalline TiO_2 electrode was immersed in a N719 dye solution for 18 h to allow chemisorption of the dye molecules. The counter electrode of the DSSC was prepared by spin coating of a H_2PtCl_6 solution on the back size of FTO substrate with CdS coated TiO_2 nanorod array and heating it at 400 °C for 30 min. Because FTO was covered on each side of the glass substrate, the generated electrons from the CdS sensitized TiO_2 nanorod array can be easily transferred to the Pt electrode.

2.4. Characterization

To examine the morphology of samples, field emission scanning electron microscopy (FE-SEM, JSM-7000F, Japan) was used. X-ray diffraction measurements were carried out for observation of crystalline phase with a Siemens diffractometer D500/5000 in Bragg–Brentano geometry under Cu K radiation. Also, optical properties are investigated using a UV–vis spectrophotometer (UV-2401 PC, Shimadzu).

2.5. Photoelectrochemical measurements

The electrochemical properties were investigated using 3-electrode configuration with Pt as a counter electrode and Ag/AgCl reference electrode (CH Instruments, CHI 660) in 0.35 M Na_2SO_3 and 0.24 M Na_2S aqueous solution as electrolytes. Linear sweep voltametry technique was used at a scan rate of 10 mV s^{-1}. The working electrode was illuminated with a 150 W xenon lamp based solar simulator (PECCELL, Yokohama, Japan, PEC-L01:100 mW cm^{-2}) of which light intensity was calibrated using

a silicon reference cell (Fraunhofer ISE, Certificate No. C-ISE269). The measured light irradiance was 100 mW cm^{-2}.

3. Results and discussion

Fig. 2(a) shows a typical morphology of the synthesized TiO_2 nanorod arrays on FTO substrate. It was found that the top shape of hydrothermally grown TiO_2 nanorod was square, and all TiO_2 nanorods were well aligned and their average diameter and length were about 55–75 nm and 400 nm, respectively. Also, we can see about 50 nm inter-nanorod distance that can supply a void for the doping materials that were determined from FESEM and TEM images (Figs. 2(b),(c) and 4(a)). The TiO_2 nanorods are perpendicular to the substrate and well aligned. Examination of selected area electron diffraction (SAED) pattern shows that the nanorods are single crystalline (Fig. 4(b)). The TiO_2 phase was rutile, which had 3.4 Å d-space as can be seen Fig. 4(a) inset image, showing that is in a good agreement with the rutile TiO_2 (110) lattice spacing of 3.247 Å.

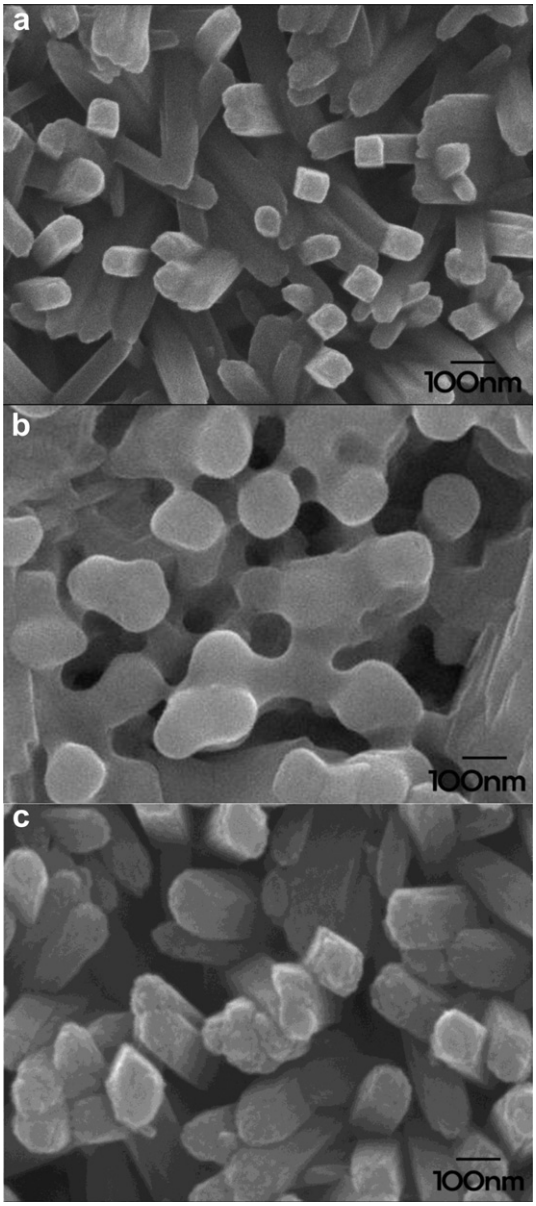

Fig. 2. FESEM images of (a) TiO_2 nanorod arrays, and CdS nanoparticles deposited on the TiO_2 nanorod arrays from (b) electrodeposition method (c) spray pyrolysis method.

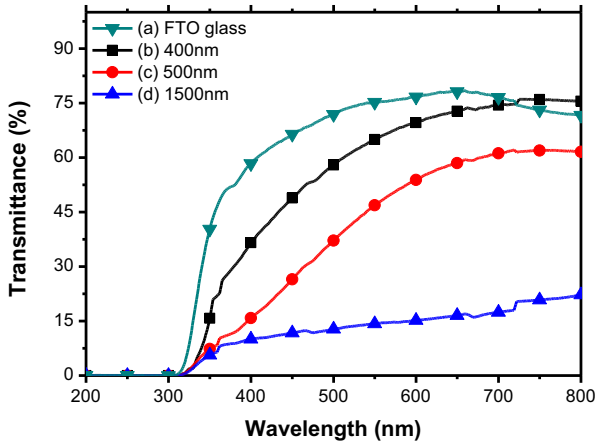

Fig. 3. Transmittance spectra of (a) bare FTO glass, and hydrothermally grown TiO_2 nanorod arrays on FTO with (b) 400 nm, (c) 500 nm and (d) 1500 nm rod length.

Fig. 3 shows the transmittance spectra of (a) a bare FTO glass, (b) the TiO_2 nanorod with 400 nm rod length, (c) the TiO_2 nanorod with 500 nm rod length and (d) the TiO_2 nanorod with 1500 nm rod length. The maximum transmittance intensity of the bare FTO substrate is about 78%. As we increase the TiO_2 rod length, the nanostructure can enlarge the specific surface area of TiO_2 that can act as scaffold for the hybridization with low-bandgap material to increase the photon production. However, as the rod length was increased, the films became opaque. In the view point of conduction energy band of TiO_2, the photogenerated electrons can participate in water reduction to make hydrogen. However, more external bias should be applied to maximize the solar-to-hydrogen conversion efficiency. Thus, several metal oxide based PECs have been combined with other energy generating systems such as dye-sensitized solar cell or Si solar cell [27–29]. To use a photoanode for hybrid tandem system, transparency of the photoanode is highly required because relatively long-wavelength solar light has to be harvested by other energy generating device located behind the photoanode. Therefore, it is obvious that the 400 nm rod length is suitable as a photoanode in the tandem cell.

We prepared CdS coated TiO_2 nanorod arrays by using two different deposition methods. Fig. 2(b) and (c) show top-view SEM image of CdS nanoparticles decorated TiO_2 nanorod arrays by electrodeposition method and by spray pyrolysis deposition, respectively. CdS layers grown by electrodeposition method were aggregated film on the TiO_2 top and wall surfaces, and well covered on each TiO_2 nanorod array. As it can be seen in Fig. 2(c), the diameters of the composite nanorod arrays increased from 65 to 135 nm, which corresponds to the film thickness of the CdS layers. In the case of CdS deposited by spray pyrolysis deposition method, the TiO_2 surface was uniformly covered with CdS nanoparticles, with a diameter range about 12–18 nm (Fig. 4(c)).

The UV/visible light absorption spectra of TiO_2, CdS/TiO_2 samples coated by two different methods, electrodeposition and spray pyrolysis deposition, are shown in Fig. 5. In these data, the TiO_2 nanorod arrays can absorb from 410 nm wavelength, which corresponds to the bandgap of the rutile phase TiO_2. Two CdS/TiO_2 samples indicate different light absorption edges. The larger particles of CdS prepared by electrodeposition method can absorb the longer wavelength energy than the CdS smaller particles by spray pyrolysis deposition due to the quantum confinement effects [30,31].

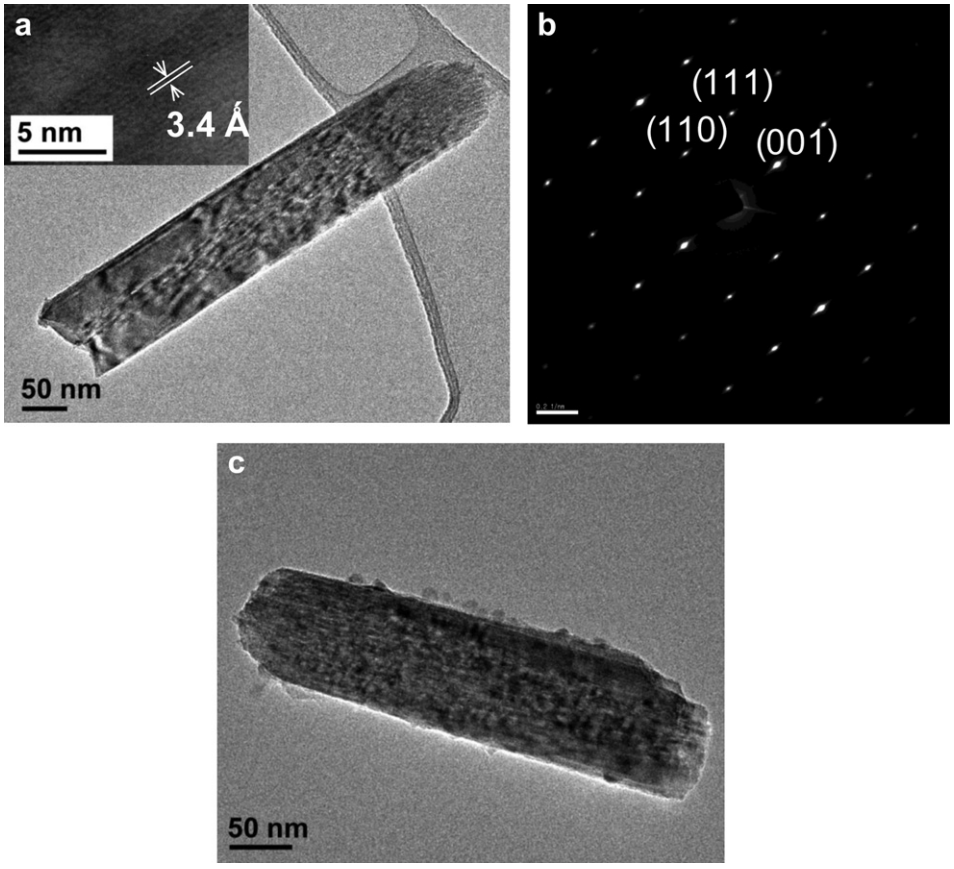

Fig. 4. TEM image (a), high resolution TEM image (a, inset) SAED pattern (b) of TiO_2 nanorod, and TEM image of CdS particles deposited TiO_2 nanorod from spray pyrolysis deposition method (c).

The photoelectrochemical responses of TiO_2 and CdS/TiO_2 composite samples from different deposition methods are shown in Fig. 6. Hydrothermally grown TiO_2 nanorod array shows little photocurrent density, in which the maximum value was 0.03 mA cm^{-2} when the external bias of 0.2 V vs. Ag/AgCl was applied. However, CdS/TiO_2 composite photoanodes show greatly increased photocurrent values, where spray pyrolysis is better than the electrochemical deposition method. The fine particle size of CdS from the spray pyrolysis deposition is considered the main reason for the superior photo-responses regardless of their higher bandgap energy. In the case of the CdS particles prepared from the electrochemical deposition method, the film type morphology decreased contact area with the electrolyte, causing the ineffective split of the excited electron and hole pairs.

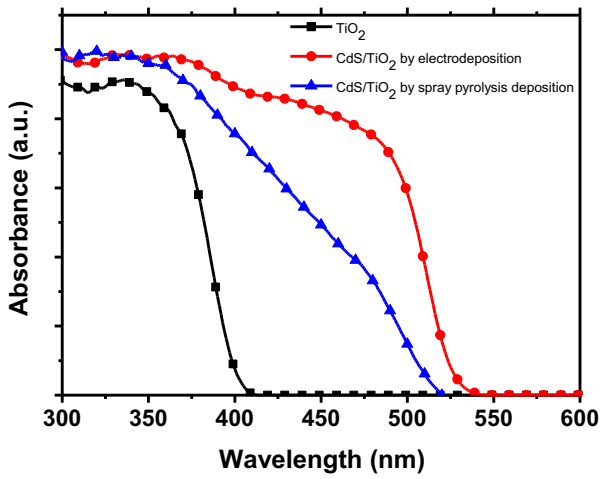

Fig. 5. UV/VIS absorption spectra of TiO_2 nanorods (square symbol), CdS nanoparticles coated TiO_2 nanorods from electrodeposition (circular symbol), and that from spray pyrolysis deposition (triangular symbol).

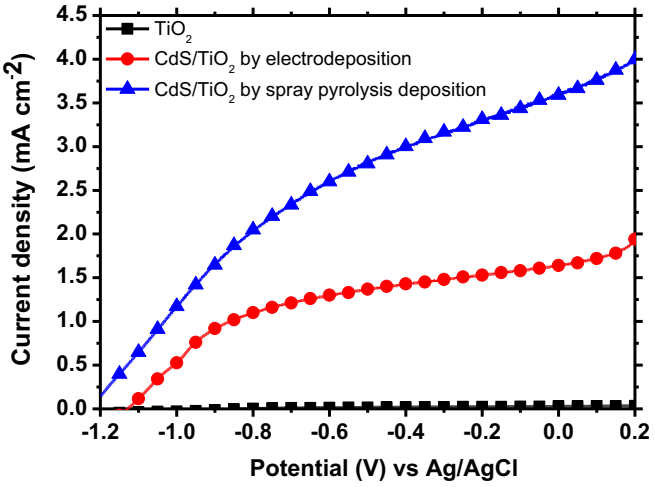

Fig. 6. Linear sweep voltammograms of TiO_2 (square symbol), TiO_2/CdS deposited by electrodeposition (circular symbol), and by spray pyrolysis deposition (triangular symbol) used as photoanodes under 100 mW cm^{-2} illumination.

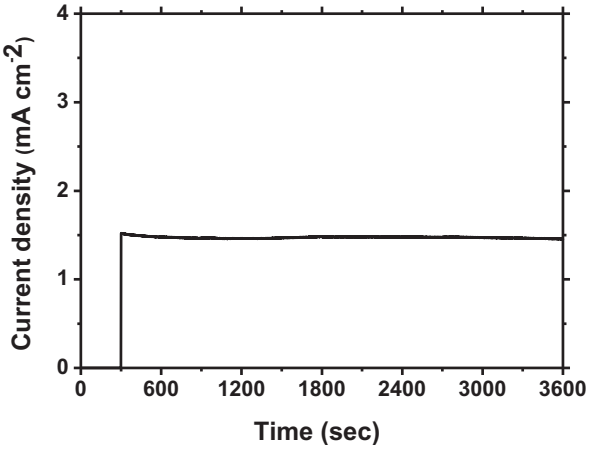

Fig. 7. Current versus time measurements of CdS nanoparticles coated TiO_2 nanorod from electrodeposition at −0.2 V (vs. Ag/AgCl) bias.

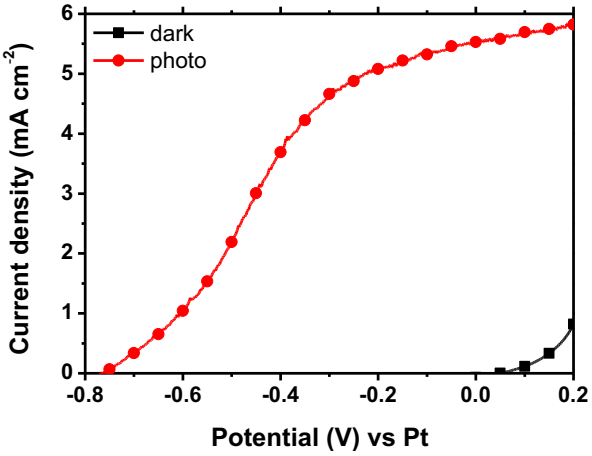

Fig. 9. The I–V curve of the CdS/TiO_2 nanocomposite/DSSC tandem cell under 100 mW cm^{-2} illumination.

The photocurrent versus time was examined to confirm stability of CdS coated TiO_2 nanorod arrays as a photoanode under 1 sun illumination (Fig. 7). During 1 h measurement, −0.2 V (vs. Ag/AgCl) of external bias was applied to the photoanode. There is no significant photocurrent degradation after about 1 h illumination, showing good electrochemical stability in hole scavenger electrolyte including Na_2S and Na_2SO_3.

To make the unassisted water splitting system, CdS/TiO_2 composite electrode was connected with Pt counter electrode of dye-sensitized solar cell [32]. Before making the tandem cell, transmittance spectra of the samples were measured (Fig. 8). A photoanode, which is suitable for being comprised of tandem cell, should be highly transparent at the 730 nm wavelength region for light absorption of dye molecules. The CdS/TiO_2 nanocomposite materials from spray pyrolysis deposition were shown 36% of transmittance. A FTO glass, which is usually used as a substrate in the dye-sensitized solar cells, was shown 74% of transmittance. Even though 36% of incident solar light can reach the dye-sensitized TiO_2 electrode, it could be considered suitable for fabrication of PEC/PV tandem cell in the view point of current matching between the CdS/TiO_2 electrode and dye-sensitized TiO_2 electrode.

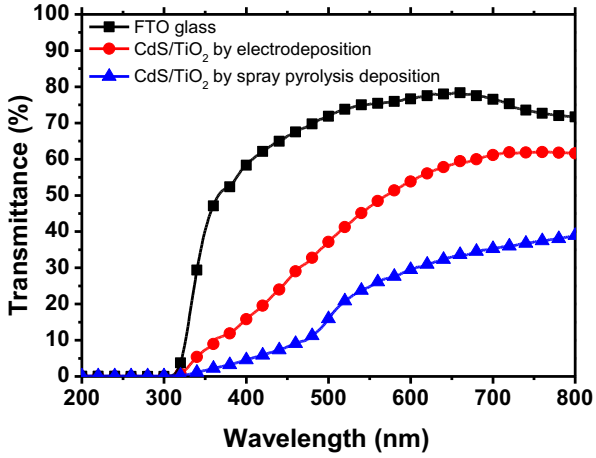

Fig. 8. UV/VIS transmittance spectra of TiO_2 nanorod (square symbol), CdS nanoparticles coated TiO_2 nanorod from electrodeposition (circular symbol), and that from spray pyrolysis deposition (triangular symbol).

In Fig. 9, the photocurrent response of the PEC/PV tandem cell is shown. The photoelectrochemical response was measured in the 2-electrode system, counter and reference electrode were platinum foils, and the photoanode connected DSSC was the working electrode. The measured photocurrent density was approximately 5.5 mA cm^{-2} at the zero bias potential, which indicates the maximum short-circuit current and the operating point of tandem cell in water splitting system without externally applied bias. The photocurrent value of tandem cell is about 1.6 times higher than that of photoanode at the zero potential.

4. Conclusions

The visible light sensitive photoanodes were successfully fabricated using CdS nanoparticles sensitized TiO_2 nanorod arrays grown on FTO substrate for application of photoelectrochemical cell. Two different ways of CdS deposition, which are electrochemical wet method and spray pyrolysis deposition method, were carried out and their optical, photoelectrochemical responses were investigated. The larger particles of CdS from electrodeposition showed relatively lower photocurrent density than that of spray pyrolysis deposition. Therefore, we prepared photoanode/DSSC tandem cell by using a bipolar CdS coated TiO_2 nanorod and Pt electrode connected with a dye-coated TiO_2 electrode through an iodine/triiodide electrolyte. Since the tandem cell can be provided with extra bias itself, we believe that it can be a promising way to increase photocurrent density.

Acknowledgment

This work was supported by an NRF grants funded by the Korea Ministry of Education, Science and Technology (MEST) (NRF-2009-C1AAA001-2009-0094157, the NCRC program (2011-0006268) and the Hydrogen Energy R&D Center (21st Century Frontier R&D Program)). This work was also partially supported by the New and Renewable Energy Program through the KETEP funded by the Ministry of Knowledge Economy (MKE) (008NPV08J010000).

References

[1] A. Fujishima, K. Honda, Nature 238 (1972) 37–38.
[2] A.J. Nozik, Nature 257 (1975) 383–386.
[3] A. Fujishima, X.T. Zhang, D.A. Tryk, Sur. Sci. Rep. 63 (2008) 515–582.
[4] X. Yang, A. Wolcott, G. Wang, A. Sobo, R.C. Fitzmorris, F. Qian, J.Z. Zhang, Y. Li, Nano Lett. 9 (2009) 2331–2336.

[5] K.S. Ahn, S. Shet, T. Deutsch, C.S. Jiang, Y.F. Yan, M. Al-Jassim, J. Turner, J. Power Sources 176 (2008) 387–392.
[6] A. Enesca, A. Duta, J. Schoonman, Thin Solid Films 515 (2007) 6371–6374.
[7] B. Yang, P.R.F. Barnes, Y. Zhang, Catal. Lett. 118 (2007) 280–284.
[8] K. Sivula, R. Zboril, F.L. Formal, R. Robert, A. Weidenkaff, J. Tucek, J. Frydrych, M. Gratzel, J. Am. Chem. Soc. 132 (2010) 7436–7444.
[9] V.R. Satsangi, S. Kumari, A.P. Singh, R. Shrivastav, S. Dass, Int. J. Hydrogen Energy 33 (2008) 312–318.
[10] C. Burda, Y. Lou, X. Chen, A.C.S. Samia, J. Stout, J.L. Gole, Nano Lett. 3 (2003) 1049–1051.
[11] C.J. Lin, Y.T. Lu, C.H. Hsieh, S.H. Chien, Appl. Phys. Lett. 94 (2009) 113102.
[12] J.J. Wu, C.C. Yu, J. Phys. Chem. B 108 (2004) 3377–3379.
[13] J.-M. Wu, H.C. Shih, Y.-K. Tseng, C.-L. Hsu, C.-Y. Tsay, J. Electrochem. Soc. 154 (2007) H157–H160.
[14] X. Feng, K. Shankar, O.K. Varghese, M. Paulose, T.J. Latempa, C.A. Grimes, Nano Lett. 8 (2008) 3781–3786.
[15] M. Adachi, Y. Murata, J. Takao, J.T. Jiu, M. Sakamoto, F.J. Wang, J. Am. Chem. Soc. 126 (2004) 14943–14949.
[16] G.K. Mor, K. Shankar, M. Paulose, O.K. Varghese, C.A. Grimes, Nano Lett. 5 (2005) 191–195.
[17] Q.H. Zhang, L. Gao, Langmuir 19 (2003) 967–971.
[18] Q.A. Shen, D.T. Toyoda, J. Photochem. Photobiol. A Chem. 164 (2004) 75–80.
[19] B. Liu, E.S. Aydil, J. Am. Chem. Soc. 131 (2009) 3985–3990.
[20] S.S. Srinivasan, J. Wade, E.K. Stefanakos, J. Nanomater. (2006) 87326.
[21] D.R. Baker, P.V. Kamat, Adv. Funct. Mater. 19 (2009) 805–811.
[22] W. Ho, J.C. Yu, J. Mol. Catal. A Chem. 247 (2006) 268–274.
[23] I. Robel, V. Subramanian, M. Kuno, P.V. Kamat, J. Am. Chem. Soc. 128 (2006) 2385–2393.
[24] J.Y. Kim, S.B. Choi, J.H. Noh, S.H. Yoon, S. Lee, T.H. Noh, A.J. Frank, K.S. Hong, Langmuir 25 (2009) 5348–5351.
[25] S. Banerjee, S.K. Mohapatra, P.P. Das, M. Misra, Chem. Mater. 20 (2008) 6784–6791.
[26] K. Shin, S.I. Seok, S.H. Im, J.H. Park, Chem. Commun. 46 (2010) 2385–2387.
[27] Y. Yamada, N. Matsuki, T. Ohmori, H. Kondo, A. Matsuda, E. Suzuki, Int. J. Hydrogen Energy 28 (2003) 1167–1169.
[28] E.L. Miller, M. Marsen, D. Paluselli, R. Rocheleau, Electrochem. Solid-State Lett. 8 (2005) A247–A249.
[29] J.H. Park, A.J. Bard, Electrochem. Solid-State Lett. 9 (2006) E5–E8.
[30] B. Zorman, M.V. Ramakrishna, R.A. Friesner, J. Phys. Chem. 99 (1995) 7649–7653.
[31] T.V. Buuren, L.N. Dinh, L.L. Chase, W.J. Siekhaus, L.J. Terminello, Phys. Rev. Lett. 80 (1998) 3803–3806.
[32] J.K. Kim, K. Shin, S.M. Cho, T.W. Lee, J.H. Park, Energy Environ. Sci. 4 (2011) 1465–1470.